Наносистеми, наноматеріали, нанотехнології
Nanosistemi, Nanomateriali, Nanotehnologii
2025, т. 23, № 1, сс. 177–189
https://doi.org/10.15407/nnn.23.01.0177

PACS numbers: 72.80.Tm, 77.22.Ch, 77.22.Gm, 78.30.Jv, 81.07.Pr, 82.35.Np

Effect of WC-Nanoparticles' Addition on the Structural and Dielectric Characteristics of a Biopolymer

Majeed Ali Habeeb[1], Idrees Oreibi[2], Rehab Shather Abdul Hamza[1], Dhay Ali Subar[1], and Khalid Al-ammar[1]

[1]*College of Education for Pure Sciences,*
Department of Physics,
University of Babylon,
Hillah, Iraq
[2]*Directorate of Education Babylon,*
Ministry of Education,
Babylon, Iraq

This study involves preparing nanocomposites consisting of polyvinyl alcohol (PVA) and tungsten carbide (WC) nanoparticles. The casting process is employed to create these nanocomposites, with varying weight percentages of WC nanoparticles: 0, 1, 2, and 3 wt.%. Various ways of diagnosis are employed to analyse the PVA–WC nanocomposites, including Fourier-transform infrared spectroscopy (FTIR), scanning electron microscopy (SEM) imaging, and optical microscopy imaging. The experimental findings obtained from the images captured by an optical microscope reveal the spatial arrangement of tungsten-carbide nanoparticles throughout all nanocomposite films. Additionally, these results demonstrate the presence of a cohesive network of ions dispersed throughout the polymer matrix, with a tungsten-carbide nanoparticles' concentration of 3 wt.%. Furthermore, the experimental findings obtained from Fourier-transform infrared spectroscopy (FTIR) demonstrate an upward trend between the absorbance values of the PVA–WC nanocomposites and the fraction of tungsten-carbide nanoparticles. The peak properties remain consistent, and most bonds exhibit similar wavenumbers. The electrical characteristics of nanocomposites are investigated in the frequency range of 100-to-$5 \cdot 10^6$ Hz at ambient temperature. The analysis of the A.C. electric properties reveals that, as the frequency of the applied electrical field increases, the dielectric constant and dielectric loss of the nanocomposites diminish. In contrast, these properties indicate an increase with tungsten-carbide nanoparticles' concentration. Additionally, the A.C. electrical conductivity of the nanocomposites displays an increase with higher concentrations of tungsten-carbide nanoparticles and frequency, while remaining relatively constant at high frequencies. The conclusive findings indicate that the

nanostructures composed of polyvinyl alcohol and tungsten carbide (PVA–WC) possess potential applications in diverse electrical and electronic nanodevices.

Це дослідження передбачає приготування нанокомпозитів, що складаються з наночастинок полівінілового спирту (PVA) і карбіду Вольфраму (WC). Процес лиття використовувався для створення цих нанокомпозитів із змінним ваговим відсотком наночастинок WC: 0, 1, 2 і 3 мас.%. Для аналізи нанокомпозитів PVA–WC використовувалися різні способи діягностики, включаючи інфрачервону спектроскопію на основі Фур'є-перетвору (FTIR), сканувальну електронну мікроскопію (SEM) та оптичну мікроскопію. Експериментальні дані, одержані із зображень за допомогою оптичного мікроскопа, показують просторове розташування наночастинок карбіду Вольфраму в усіх нанокомпозитних плівках. Крім того, ці результати демонструють наявність цілісної мережі йонів, розсіяних по всій полімерній матриці, з концентрацією наночастинок карбіду Вольфраму у 3 мас.%. Крім того, експериментальні результати, одержані за допомогою інфрачервоної спектроскопії на основі Фур'є-перетвору (FTIR), продемонстрували тенденцію до зростання між значеннями вбирання нанокомпозитами PVA–WC і часткою наночастинок карбіду Вольфраму. Властивості піку залишаються незмінними, і більшість зв'язків демонструють подібні хвильові числа. Електричні характеристики нанокомпозитів досліджували в діяпазоні частот від 100 до $5 \cdot 10^6$ Гц за температури навколишнього середовища. Аналіза властивостей змінного електричного струму показує, що зі збільшенням частоти прикладеного електричного поля діелектрична проникність і діелектричні втрати нанокомпозитів зменшуються. Навпаки, ці властивості вказують на збільшення з концентрацією наночастинок карбіду Вольфраму. Крім того, електропровідність нанокомпозитів на змінному струмі демонструє збільшення з вищими концентраціями наночастинок карбіду Вольфраму та частотою, залишаючись відносно постійною на високих частотах. Переконливі висновки показують, що наноструктури, що складаються з полівінілового спирту та карбіду Вольфраму (PVA–WC), мають потенційне застосування в різноманітних електричних та електронних нанопристроях.

Key words: PVA, WC nanoparticles, nanocomposites, electrical properties.

Ключові слова: полівініловий спирт, наночастинки WC, нанокомпозити, електричні властивості.

(Received 15 October, 2023)

1. INTRODUCTION

Polymer nanocomposites (PNCs) can be described as composite materials whereby one or more nanofillers are dispersed inside a polymer matrix. The primary objective is to integrate the ease of processing of polymers with the exceptional material properties offered

by nanofillers to create composite materials that demonstrate substantially enhanced macroscopic characteristics [1, 2]. Polymer nanocomposites (PNCs) hold significant importance in industrial and research domains, finding extensive applications in several sectors, such as packaging, transportation, safety, energy, electromagnetic shielding, catalysis, sensors, defence systems, and the information industry. Polymer nanocomposites (PNCs) can address numerous real-world difficulties and daily concerns, exhibiting promising prospects for future applications. Phenolic nanocomposites (PNCs) are formulated using the idea that increased size and surface area significantly enhance reactivity. Polymer nanocomposites (PNCs) are composite materials with polymers as the matrix and nanomaterials as the nanofillers. Polymer nanocomposites (PNCs) possess exceptional multifunctionality owing to integrating many components into a suitable and integrated structure. This unique characteristic allows PNCs to find extensive applications in diverse fields such as electronics, magnetism, and optics [3, 4]. Polyvinyl alcohol (PVA) is a significant and versatile non-ionic hydrophilic polymer that has attracted considerable interest as a hydrogel and for various other applications, predominantly due to its non-toxicity. There are two distinct ways to create polyvinyl alcohol (PVA) gels: chemical and physical methods. Chemical cross-linking of PVA hydrogels can be accomplished by utilizing multifunctional aldehyde compounds like glutaraldehyde, glyoxal, and borate-containing species or through irradiation methods such as gamma radiation. However, using a chemical cross-linker may be associated with deleterious consequences, such as undesired interactions with other constituents, if present. Physically crosslinked polyvinyl alcohol (PVA) hydrogels are commonly favoured for various applications, particularly in biotechnology, owing to their exceptional purity and ease of gelation at mild conditions [5, 6].

Transition metal carbides are important due to their desirable features, including thermal stability, resistance to corrosion and wear, and electrical, magnetic, and catalytic characteristics [7]. Due to its extraordinary electrical conductivity and favourable hydrogen-adsorption properties, tungsten carbide (WC) has attracted much interest in the scientific community [8]. Nanosize tungsten carbide (WC) has garnered significant interest within the scientific community due to its improved tribomechanical and chemical characteristics. The applicability of fuel cells has given rise to a new realm of catalytic applications in power production [9, 10]. The WC nanomaterial has been discovered to exhibit a bulk modulus comparable to that of diamond, making it suitable for utilization in high-pressure tests. A significant proportion of industrially manufactured tungsten carbide (WC) is allocated for producing cemented

carbide, which finds application in several sectors, such as cutting tools, tunnelling operations and drilling, dies, and wear-resistant components, among others [11, 12]. In a recent study, we have documented the successful production of WC nanoparticles using a solid-state reaction involving scheelite and activated charcoal. This reaction occurred under an argon atmosphere at a temperature of 1025°C [13]. Tungsten carbide (WC) is a highly challenging substance characterized by its exceptional hardness, inertness, and refractory nature.

Moreover, it has remarkable catalytic capabilities that closely resemble those of platinum. Historically, the synthesis of transition metal carbides has predominantly relied on powder metallurgical methods involving high temperatures. The techniques above exhibit high-energy consumption and yield coarse particles with reduced surface area, constraining their potential in ceramic and catalytic contexts [14, 15].

This work used tungsten carbide to improve the structural and electrical properties of nanocomposite PVA–WC. This study showed a significant improvement in these characteristics mentioned above.

2. MATERIALS AND METHODS

Polymer nanocomposite films were fabricated by dissolving pure polyvinyl alcohol (PVA) in 40 mL of distilled water for 35 minutes. The solution was stirred using a magnetic stirrer at a temperature of 60°C to enhance the uniformity of the resulting solution by summing the weight percentages of additives 0, 1, 2, and 3 wt.% of (WC), the resulting films are obtained through casting. This process entails depositing the mixture into a template, specifically a Petri dish with a diameter of 5 cm, and allowing it to dry for 3–7 days. Subsequently, the films are carefully removed from the template for the required tests. The thickness of the films is measured using a micrometre, resulting in a value of 120 μm. The technique employed in this study is Fourier-transform infrared (FTIR) spectroscopy, which is utilized to analyse nanocomposite samples consisting of polyvinyl alcohol and tungsten carbide. The spectral analysis is conducted within the 1000 to 4000 cm^{-1} wave number range. The dielectric characteristics of nanocomposites were assessed by employing an LCR meter, namely the HIOKI 3532-50 LCR HI TESTER model, which operates within a frequency range spanning from 100 Hz to 5 MHz. The materials were tested at various concentrations using an Olympus-type Nikon-73346 optical microscope. This microscope had a magnification of ×10 and was paired with a camera designed specifically for capturing microscopic images.

In order to determine the dielectric constant (ε′), one may employ

the following formula [16]:

$$\varepsilon' = C_p/C_0; \quad (1)$$

C_p represents capacitance, and C_0 represents a vacuum capacitor.

Dielectric loss (ε'') is calculated as follows [17, 18]:

$$\varepsilon'' = \varepsilon' D. \quad (2)$$

In this case, displacement D is applied.

The conductivity of A.C. electricity is computed with the following formula [19, 20]:

$$\sigma_{\text{A.C.}} = \omega\varepsilon_0\varepsilon', \quad (3)$$

where ω is the angular frequency.

3. RESULTS AND DISCUSSION

3.1. Fourier-Transform Infrared (FTIR) Analysis of PVA–WC NCs

Fourier-transform infrared (FTIR) spectroscopy is a highly valuable analytical technique that offers great insights into the interactions of functional groups within a given compound. This study conducted infrared (IR) analysis on a Fourier-transform infrared transmission profile spectrum. The purpose was to describe the interface between pure polyvinyl alcohol and its nanocomposite films, which contained varying ratios of tungsten carbide nanoparticles (WC NPs) at 1, 2, and 3 wt.%. The analysis was performed at room temperature (RT) within the 500–4000 cm^{-1} wavenumber range, as depicted in Fig. 1. The functional groups of PVA emerged at 3259, 2908, 1416, 1250, and 1084 cm^{-1}, corresponding to broadband to the stretching vibrations of hydroxyl groups O–H, methyl C–H_3 asymmetric stretching band, O–CH_3 deformation, O–H ether group bending vibration and C–O stretching vibration, respectively. The spectral bands observed at 900 cm^{-1} and within 600-to-550 cm^{-1} range are attributed to the stretching vibrations of peroxide C–O–O bonds and C–H bonds, respectively [21, 22].

Upon comparing the characteristic wavenumbers of the PVA–WC nanocomposite with those of pure PVA, it becomes evident that the distinct peaks representing the nanocomposite were not discernible; this can be attributed to the observed shifting, which can be attributed to the incorporation of WC. Moreover, it has been observed that the transmittance exhibits a drop when the ratios of tungsten carbide nanoparticles (WC NPs) grow, increasing the density of

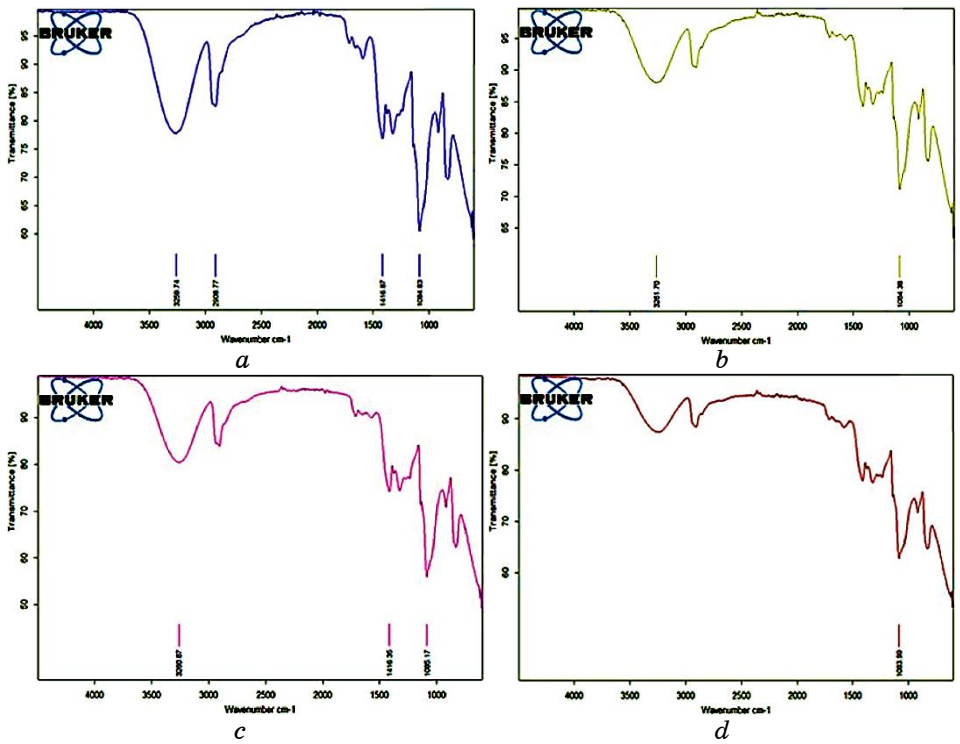

Fig. 1. FTIR spectra for PVA–WC nanocomposites: (*a*) for pure PVA; (*b*) for 1 wt.% WC; (*c*) for 2 wt.% WC; (*d*) for 3 wt.% WC.

these nanoparticles. Based on the present investigation, it can be inferred that no discernible absorption peaks were observed, indicating the absence of any notable interactions between the PVA polymer and WC NPs [23, 24].

Figure 2 displays the photomicrographs of the surface of pure polyvinyl alcohol (PVA) and its nanocomposites (NCs) containing varying weight percentages (wt.%) of tungsten carbide nanoparticles (WC NPs) at a magnification level of ×10. The schematic diagram of the polymer film in part (*a*) demonstrates a uniform composition without any distinct separation of phases. Specifically, it exhibits a refined structure with a sleek surface, indicating the remarkable compatibility of PVA at this particular mix ratio. The analysis of the figures (part *b*–*d*) reveals that the WC NPs exhibit a uniform distribution across the surface of the polymer-mix films. This observation becomes more pronounced as the weight percentage of WC increases.

The non-covalent interactions (NCs) exhibit an almost circular arrangement of particles with a consistent shape. This phenomenon

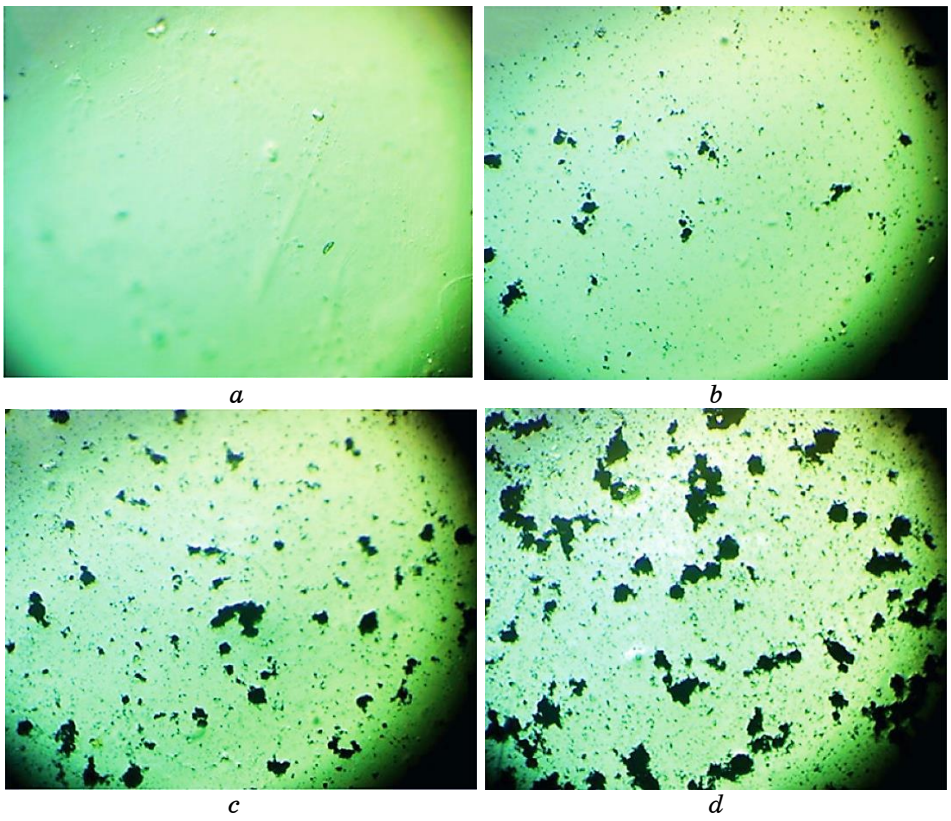

Fig. 2. Photomicrographs (×4) for PVA–WC NCs: (*a*) for pure PVA; (*b*) for 1 wt.% WC; (*c*) for 2 wt.% WC; (*d*) for 3 wt.% WC.

is attributed to the significant surface area of nanoparticles (NPs) [25, 26].

On the other hand, the polymeric solution with distinct polar groups exhibits a pronounced attraction towards WC, hence resulting in the alignment of the nanoparticles within the polymer chain. Consequently, the structural arrangement of the NC becomes denser, leading to an enhancement in the material's overall consistency. This method presented below offers an appropriate approach for developing NC films [27, 28].

Figure 3 demonstrates the influence of including WC nanoparticles on the dielectric constant of pristine polyvinyl alcohol (PVA). There is a positive association between the concentration of WC nanoparticles and the dielectric constant. The increased concentration found can be ascribed to the aggregation of WC nanoparticles within the nanocomposites when they are included at low levels. Consequently, the dielectric constant experiences a decrease, while, at el-

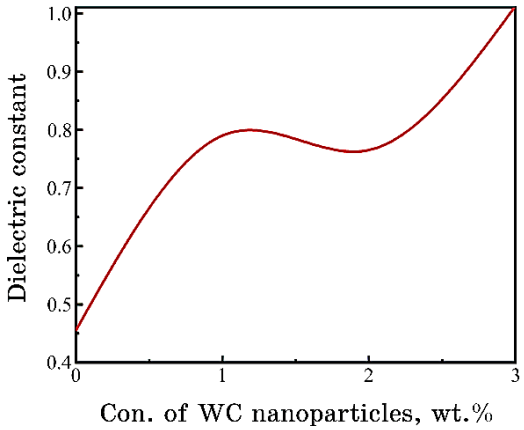

Fig. 3. Influence of WC-NPs' content on the ε′ of PVA–WC NCs at 100 Hz.

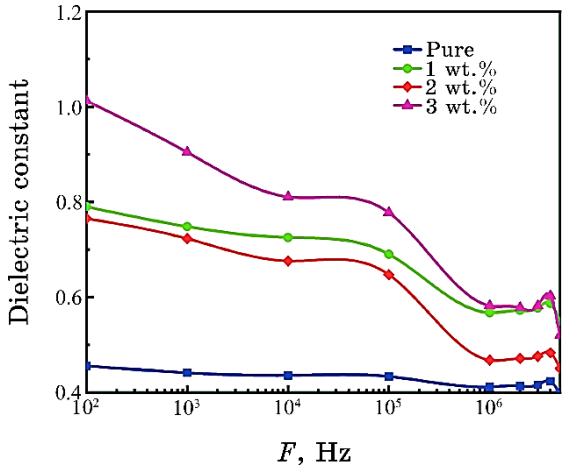

Fig. 4. Behaviour of ε′ with a frequency of PVA–WC NCs.

evated concentrations, the presence of WC nanoparticles leads to the formation of a cohesive network inside nanocomposites, thereby increasing the dielectric constant value [29, 30].

Figure 4 depicts the frequency-dependent fluctuation of the dielectric constant in nanocomposites of polyvinyl alcohol and tungsten carbide PVA–WC. The data presented in the figure indicates a decrease in the dielectric constants of the nanocomposite samples as the frequency of the applied field increases. This phenomenon can be attributed to the alignment of the dipole moments within the nanocomposite samples as they orient themselves in response to the

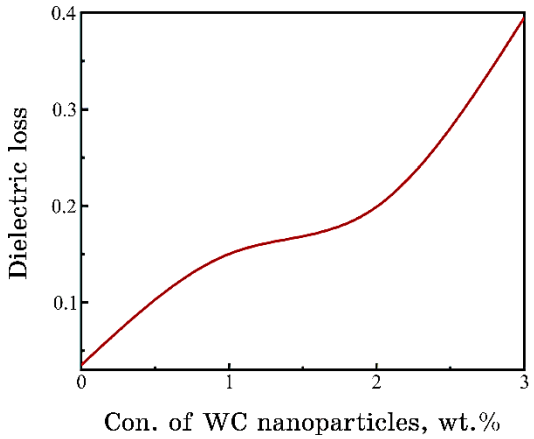

Fig. 5. Influence of WC-NPs' content on the ε″ of PVA–WC NCs at 100 Hz.

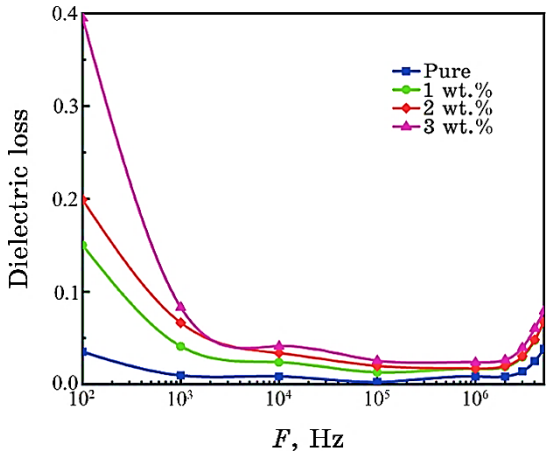

Fig. 6. Behaviour of ε″ with a frequency of PVA–WC NCs.

applied electrical fields. Consequently, this alignment reduces the polarization of the space charge, ultimately leading to a decrease in absolute polarization [31, 32].

Figure 5 illustrates the fluctuation in dielectric loss of pure polyvinyl alcohol (PVA) concerning the material's weight concentration (WC). The dielectric loss of PVA–WC nanocomposites positively correlates with the concentration of WC nanoparticles, which can be attributed to the concurrent increase in the number of charge carriers. When the concentration of nanoparticles is beyond a certain threshold, nanoparticles aggregate to create a cohesive network

within nanocomposites [33, 34].

Figure 6 depicts the dielectric loss characteristics of nanocomposites composed of polyvinyl alcohol (PVA) and tungsten carbide (WC), as influenced by frequency. The provided figure illustrates a noticeable trend in which the dielectric loss of nanocomposites decreases as the frequency of the applied electric field increases. The phenomenon can be attributed to the reduced influence of space charge polarization and the heightened dielectric loss observed in the nanocomposites comprising polyvinyl alcohol and tungsten car-

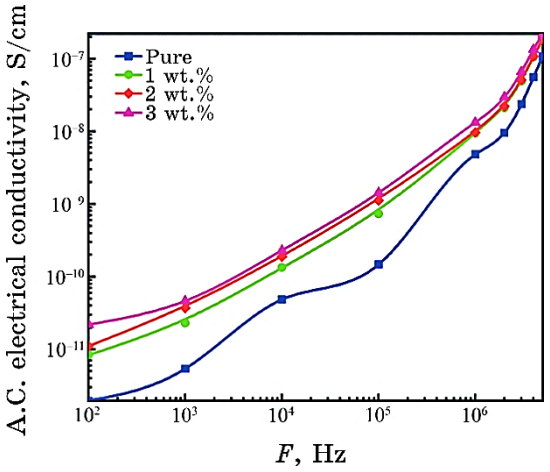

Fig. 7. Difference of conductivity for PVA–WC NCs with frequency (*F*).

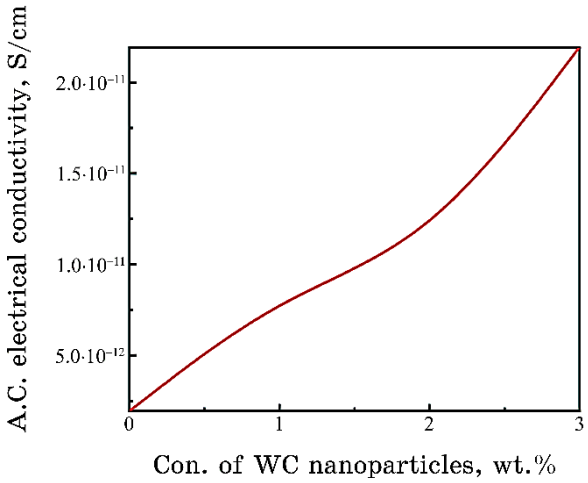

Fig. 8. Difference of electrical conductivity for PVA–WC NCs with WC-NPs' contents.

TABLE. Values of dielectric constant, dielectric loss, and A.C. electrical conductivity for PVA–WC NCs at 100 Hz.

Con. of WC NPs, wt.%	Dielectric constant	Dielectric loss	A.C. electrical conductivity, S/cm
0	0.46	0.04	$1.95 \cdot 10^{-12}$
1	0.79	0.15	$8.34 \cdot 10^{-12}$
2	0.77	0.20	$1.10 \cdot 10^{-11}$
3	1.01	0.39	$2.19 \cdot 10^{-11}$

bide PVA–WC at lower frequencies. In the present study, we aim to investigate the effects of sleep deprivation on cognitive performance [35, 36].

Figures 7 and 8 depict the performance of A.C. electrical conductivity of PVA–WC NCs as a function of frequency (*F*) and WC-NPs' concentration, respectively. The alternating current (A.C.) conductivity demonstrates a notable increase when the electric field frequency escalates across all samples. The observed phenomenon can be attributed to space charge polarization, which occurs at low frequencies, in addition to the hopping motion of charge carriers [37, 38]. Moreover, the conductivity exhibits an upward trend as the weight percentage of WC nanoparticles (NPs) increases. The observed behaviour can be attributed to the influence of space charge, which arises from the accumulation of charge carriers resulting from an increase in their regular distribution throughout the polymer matrix [39].

Table shows values of dielectric constant, dielectric loss, and A.C. electrical conductivity for PVA–WC nanocomposites at 100 Hz.

4. CONCLUSIONS

The solution cast approach was employed to deposit successfully pure polyvinyl alcohol (PVA) and its composite with varying ratios of tungsten carbide (WC).

The Fourier-transform infrared (FTIR) spectra exhibit a displacement in certain bands and alterations in the intensity of other bands compared to the spectra of pristine films. The optical microscope demonstrates high uniformity and precise integration of WC charge transfer complexes within the pure PVA sheets. The experimental results demonstrated that the dielectric constant and dielectric loss of the PVA–WC nanocomposites experienced a decrease with increasing frequency of the applied electric field. The electrical conductivity of alternating current (A.C.) positively correlates with the current frequency.

The decisive results suggest that the nanostructures composed of PVA–WC possess promising prospects for utilization in a wide range of electrical and electronic nanodevices.

REFERENCES

1. Mohamed S. A. Darwish, Mohamed H. Mostafa, and Laila M. Al-Harbi, *International Journal of Molecular Sciences*, **23**, No. 3: 1023 (2022); https://doi.org/10.3390/ijms23031023
2. Q. M. Jebur, A. Hashim, and M. A. Habeeb, *Egyptian Journal of Chemistry*, **63**: 719 (2020); doi:10.21608/ejchem.2019.14847.1900
3. M. A. Habeeb and Z. S. Jaber, *East European Journal of Physics*, **4**: 176 (2022); doi:10.26565/2312-4334-2022-4-18
4. M. A. Habeeb, *European Journal of Scientific Research*, **57**, No. 3: 478 (2011).
5. A. H. Hadi and M. A. Habeeb, *Journal of Mechanical Engineering Research and Developments*, **44**, No. 3: 265 (2021); https://jmerd.net/03-2021-265-274
6. P. G. Li, M. Lei, Z. B. Sun, L. Z. Cao, Y. F. Guo, X. Guo, and W. H. Tang, *Journal of Alloys and Compounds*, **430**, No. 1: 237 (2007); https://doi.org/10.1016/j.jallcom.2006.04.070
7. N. Hayder, M. A. Habeeb, and A. Hashim, *Egyptian Journal of Chemistry*, **63**: 577 (2020); doi:10.21608/ejchem.2019.14646.1887
8. S. M. Mahdi and M. A. Habeeb, *Optical and Quantum Electronics*, **54**, Iss. 12: 854 (2022); https://doi.org/10.1007/s11082-022-04267-6
9. Kh. G. Kirakosyan, Kh. V. Manukyan, S. L. Kharatyan, and R. A. Mnatsakanyan, *Materials Chemistry and Physics*, **110**, No. 3: 454 (2008); https://doi.org/10.1016/j.matchemphys.2008.03.003
10. M. A. Habeeb, A. Hashim, and N. Hayder, *Egyptian Journal of Chemistry*, **63**: 709 (2020); https://dx.doi.org/10.21608/ejchem.2019.13333.1832
11. A. Hashim, M. A. Habeeb, and Q. M. Jebur, *Egyptian Journal of Chemistry*, **63**: 735 (2020); https://dx.doi.org/10.21608/ejchem.2019.14849.1901
12. S. M. Mahdi and M. A. Habeeb, *Physics and Chemistry of Solid State*, **23**, No. 4: 785 (2022); doi:10.15330/pcss.23.4.785-792
13. Shawna Nations, Monique Long, Mike Wages, Jonathan D. Maul, Christopher W. Theodorakis, and George P. Cobb, *Chemosphere*, **135**: 166 (2015); https://doi.org/10.1016/j.chemosphere.2015.03.078
14. M. A. Habeeb and W. S. Mahdi, *International Journal of Emerging Trends in Engineering Research*, **7**, No. 9 : 247 (2019); doi:10.30534/ijeter/2019/06792019
15. M. A. Habeeb and R. S. Abdul Hamza, *Journal of Bionanoscience*, **12**, No. 3: 328 (2018); https://doi.org/10.1166/jbns.2018.1535
16. Shruti Nambiar and John T. W. Yeow, *ACS Applied Materials & Interfaces*, **4**, No. 11: 5717 (2012); https://doi.org/10.1021/am300783d
17. M. A. Habeeb, A. Hashim, and N. Hayder, *Egyptian Journal of Chemistry*, **63**: 697 (2020); https://dx.doi.org/10.21608/ejchem.2019.12439.1774
18. M. A. Habeeb and W. K. Kadhim, *Journal of Engineering and Applied Sciences*, **9**, No. 4: 109 (2014); doi:10.36478/jeasci.2014.109.113

19. M. A. Habeeb, *Journal of Engineering and Applied Sciences*, **9**, No. 4: 102 (2014); doi:10.36478/jeasci.2014.102.108
20. Hyeon Jeong Park, Arash Badakhsh, Ik Tae Im, Min-Soo Kim, and Chan Woo Park, *Applied Thermal Engineering*, **107**: 907 (2016); https://doi.org/10.1016/j.applthermaleng.2016.07.053
21. S. M. Mahdi and M. A. Habeeb, *Digest Journal of Nanomaterials and Biostructures*, **17**, No. 3: 941 (2022); https://doi.org/10.15251/DJNB.2022.173.941
22. A. H. Hadi and M. A. Habeeb, *Journal of Physics: Conference Series*, **1973**, No. 1: 012063 (2021); doi:10.1088/1742-6596/1973/1/012063
23. Q. M. Jebur, A. Hashim, and M. A. Habeeb, *Egyptian Journal of Chemistry*, **63**, No. 2: 611 (2020); https://dx.doi.org/10.21608/ejchem.2019.10197.1669
24. Bahaa Hussien Rabee and Idrees Oreibi, *Bulletin of Electrical Engineering and Informatics*, **7**, No. 4: 538 (2018); https://doi.org/10.11591/eei.v7i4.924
25. M. A. Habeeb and A. H. Mohammed, *Optical and Quantum Electronics*, **55**, Iss. 9: 791 (2023); https://doi.org/10.1007/s11082-023-05061-8
26. M. H. Dwech, M. A. Habeeb, and A. H. Mohammed, *Ukr. J. Phys.*, **67**, No. 10: 757 (2022); https://doi.org/10.15407/ujpe67.10.757
27. R. S. Abdul Hamza and M. A. Habeeb, *Optical and Quantum Electronics*, **55**, Iss. 8: 705 (2023); https://doi.org/10.1007/s11082-023-04995-3
28. Morget Martin, Neena Prasad, Muthu Mariappan Sivalingam, D. Sastikumar, and Balasubramanian Karthikeyan, *Journal of Material Science: Material in Electronics*, **29**: 365 (2018); https://doi.org/10.1007/s10854-017-7925-z
29. M. A. Habeeb and W. H. Rahdi, *Optical and Quantum Electronics*, **55**, Iss. 4: 334 (2023); https://doi.org/10.1007/s11082-023-04639-6
30. R. Dalven and R. Gill, *J. Appl. Phys.*, **38**, No. 2: 753 (1967); doi:10.1063/1.1709406
31. M. A. Habeeb and R. S. A. Hamza, *Indonesian Journal of Electrical Engineering and Informatics*, **6**, No. 4: 428 (2018); doi:10.11591/ijeei.v6i1.511
32. A. Goswami, A. K. Bajpai, and B. K. Sinha, *Polym. Bull.*, **75**, No. 2: 781 (2018); https://doi.org/10.1007/s00289-017-2067-2
33. A. A. Mohammed and M. A. Habeeb, *East European Journal of Physics*, **2**: 157 (2023); doi:10.26565/2312-4334-2023-2-15
34. O. E. Gouda, S. F. Mahmoud, A. A. El-Gendy, and A. S. Haiba, *Indonesian Journal of Electrical Engineering*, **12**, No. 12: 7987 (2014); https://doi.org/10.11591/telkomnika.v12i12.6675
35. H. Chandrakala, B. Ramaraj, and G. Madhu, *Journal of Alloys and Compounds*, **551**: 531 (2013); https://doi.org/10.1016/j.jallcom.2012.10.188
36. N. K. Al-Sharifi and M. A. Habeeb, *East European Journal of Physics*, **2**: 341 (2023); doi:10.26565/2312-4334-2023-2-40
37. N. Tran, A. Mir, D. Mallik, A. Sinha, S. Nayar, and T. J. Webster, *Int. J. Nanomedicine,* **5**: 277 (2010).
38. Z. S. Jaber, M. A. Habeeb, and W. H. Radi, *East European Journal of Physics*, **2**: 228 (2023); doi:10.26565/2312-4334-2023-2-25
39. S. M. Mahdi and M. A. Habeeb, *AIMS Materials Science*, **10**, No. 2: 288 (2023); doi:10.3934/matersci.2023015